BIFURCATIONS IN SYMMETRICALLY COUPLED HODGKIN-HUXLEY EQUATIONS

ISABEL S. LABOURIAU, CARLA M. A. PINTO

June 11, 2003

1. Introduction

This paper studies the bifurcation of two Hodgkin-Huxley equations coupled symmetrically in the first variable as follows:

$$\mathbf{CHH} = \begin{cases} \dfrac{dv}{dt} &= f(v,y) - \frac{k}{2}(v-u) - I \\ \dfrac{dy_j}{dt} &= \Phi\left(\gamma_j(v) - y_j\right)\tau_j(v) \\ \dfrac{du}{dt} &= f(u,z) - \frac{k}{2}(u-v) - I \\ \dfrac{dz_j}{dt} &= \Phi\left(\gamma_j(u) - z_j\right)\tau_j(u) \end{cases}$$

where f is the expression for the dynamics of the electric potential, I is the stimulus intensity, γ_j and τ_j give the dynamics for the ionic channels and Φ is the temperature compensating factor, in a Hodgkin-Huxley system, with the parameters of [9] (see also [11], [13] for notation).

The coupled system **CHH** is symmetric (see [6, 7, 1] for more information on symmetries). The group of symmetries of **CHH** is $\mathbf{Z}_2$, generated by the permutation of the two cells.

Periodic solutions $Y(t)$ of **CHH** may also have *spatio-temporal symmetries*, of the form (δ, S), with δ an orthogonal linear map, $S \in \mathbf{R}$, acting by $(\delta, S)\cdot Y(t) = \delta Y(t+S)$ ([1], [2], [7]).

Any equilibrium solution of **CHH** satisfies $y_j = \gamma_j(v)$ and $z_j = \gamma_j(u)$. For a given value $\lambda \in \mathbf{R}$ there is always a value of stimulus intensity I for which there is a *symmetric equilibrium*, where $v = u = \lambda$, given by $I = F(\lambda) = f(\lambda, \gamma(\lambda))$, with $\gamma = (\gamma_1, \gamma_2, \gamma_3)$. In this paper we use λ as a bifurcation parameter, instead of I. This simplifies some calculations but reverses the bifurcation diagrams, since $\lambda \mapsto F(\lambda)$ is a decreasing function (see section 2 below).

The set of *symmetric solutions* (with $v = u$ and $y_j = z_j$) is invariant under the flow of **CHH**. For k large enough this set is a global hyperbolic attractor for the flow [12].

The linearization of **CHH** around the symmetric equilibrium is given by:

$$L = \begin{pmatrix} H - \frac{k}{2}J & \frac{k}{2}J \\ \\ \frac{k}{2}J & H - \frac{k}{2}J \end{pmatrix} \qquad J = \begin{pmatrix} 1 & 0 & 0 & 0 \\ 0 & 0 & 0 & 0 \\ 0 & 0 & 0 & 0 \\ 0 & 0 & 0 & 0 \end{pmatrix}$$

where H is the matrix of the linearized decoupled system. Taking coordinates of the form (X, X) and $(X, -X)$, $X \in \mathbf{R}^4$, $X = (v, y_1, y_2, y_3)$, changes the matrix to block-diagonal form:

$$\begin{pmatrix} H & 0 \\ 0 & H - kJ \end{pmatrix}$$

The subspace of vectors of the form $(X, -X)$ is not invariant for the nonlinear equations **CHH**, whereas the space of symmetric solutions (X, X) is invariant for both **CHH** and its linearization.

Let $P_c(x) = x^4 + c_3x^3 + c_2x^2 + c_1x + c_0$ and $x^4 + b_3x^3 + b_2x^2 + b_1x + b_0$ be the characteristic polynomials of $H - kJ$ and H, respectively. Their coefficients are related by:

$$c_o = b_o + kd_0 \qquad c_1 = b_1 + kd_1 \qquad c_2 = b_2 + kd_2 \qquad c_3 = b_3 + k$$

where the d_j are given by:

$$d_0 = \Phi^3\tau_1(\lambda)\tau_2(\lambda)\tau_3(\lambda) \qquad d_2 = \Phi(\tau_1(\lambda) + \tau_2(\lambda) + \tau_3(\lambda))$$

and

$$d_1 = \Phi^2\left(\tau_1(\lambda)\tau_2(\lambda) + \tau_2(\lambda)\tau_3(\lambda) + \tau_1(\lambda)\tau_3(\lambda)\right).$$

Note that the d_j can all be written in the form $\Phi^{3-j}C$ where C does not depend on Φ, and that b_0 and c_0 can also be written in the form Φ^3C.

2. Steady-state bifurcations

In this section we treat the bifurcation of equilibria of **CHH**. The graph of $F(\lambda)$ in figure 1 was computed with **Maple** and shows that for a given λ, there is always some value of I for which there is a symmetric equilibrium, as remarked in section 1. Conversely, for each choice of I there is exactly one symmetric equilibrium of **CHH**.

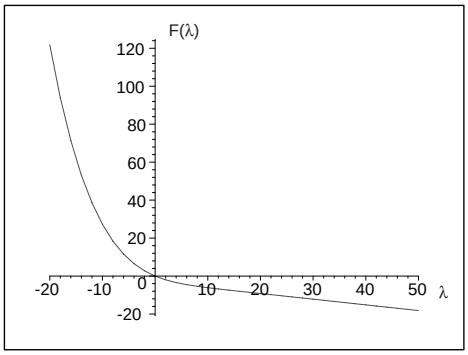

Figure 1. Graph of $I = f(\lambda, y(\lambda)) = F(\lambda)$, Hodgkin-Huxley values of the parameters.

Local bifurcations at a symmetric equilibrium takes place when the linearization at that point has a zero eigenvalue. In the notation of section 1, this happens when either $b_0(\lambda) = 0$ (eigenvalues of H) or $c_0(\lambda) = b_0(\lambda) - kd_0(\lambda) = 0$ (eigenvalues of $H - kJ$). Thus, a zero eigenvalue occurs for $k = -b_0(\lambda)/d_0(\lambda) = K(\lambda)$. That this expression is independent of Φ follows from the remarks at the end of section 1 and therefore this analysis does not depend on the temperature T.

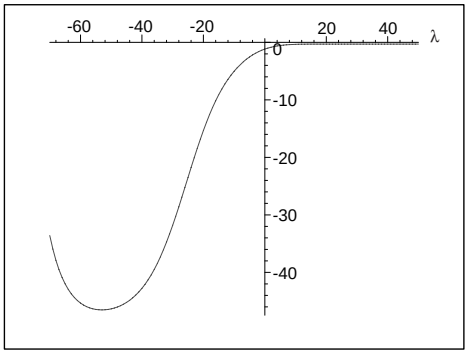

FIGURE 2. Plot of the curve $k = K(\lambda)$ where $H - kJ$ has zero eigenvalues for all temperatures, Hodgkin-Huxley values of the parameters.

The graph of $k = K(\lambda) = b_0(\lambda)/d_0(\lambda)$ is shown in figure 2, and was computed using a program written in **C**. The graph of $K(\lambda)$ never crosses the $k = 0$ axis in the range tested. This confirms the fact that no bifurcation of equilibria takes place inside the subspace of symmetric solutions , since $K(\lambda)$ is zero precisely when $b_0(\lambda) = 0$, i.e. when the matrix H has a zero eigenvalue. Thus, local bifurcations that take place at points $(\lambda, K(\lambda))$ give rise to equilibria outside the space of symmetric solutions.

Asymmetric equilibria of **CHH** can be computed directly as points $(v, y, u, z) = (x_1, \gamma(x_1), x_2, \gamma(x_2))$, with $x_1 \neq x_2$, satisfying:

$$F(x_2) - kx_2 = F(x_1) - kx_1 \tag{1}$$

and

$$F(x_2) - \frac{k}{2}(x_2 - x_1) = I = F(\lambda) \tag{2}$$

where $F(x) = f(x, \gamma(x))$. From the symmetry it follows that $x_1 = u$, and $x_2 = v$ will also determine an equilibrium for the same value of the bifurcation parameter.

For fixed values of k, a **Maple** program was used to obtain numerically a bifurcation diagram, i.e., the graph of points (λ, x_1) where there is $x_2 \neq x_1$ satisfying (1) and (2). Examples are shown in figures 7–10. We have found the types of persistent diagrams of figure 3, that we describe below, in each case giving the approximate range in k for which it can be found. The precision in the limiting values of k depends on the method used for its calculation, that will be discussed in 2.2 below, but all digits given are correct. When we have an analytic expression for the transition value of k, it is given, with the justification appearing later.

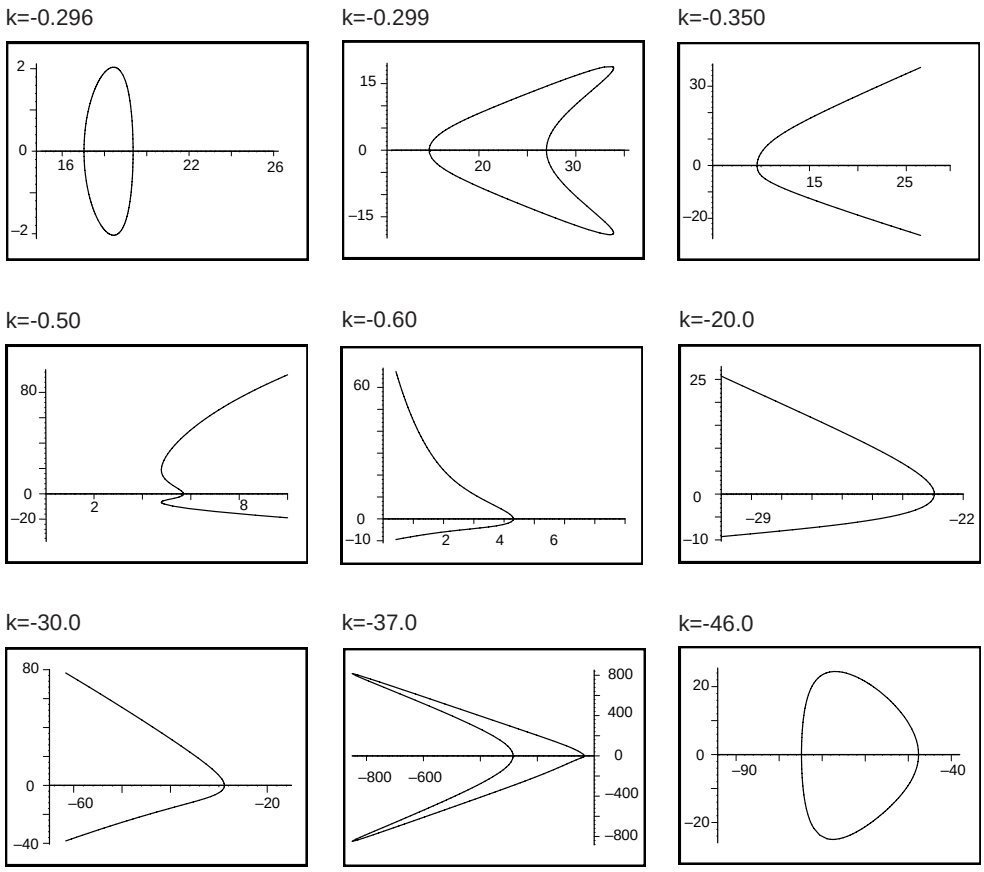

FIGURE 3. Steady-state bifurcation for **CHH**: asymmetric equilibrium $(\lambda, x) = (\lambda, v - \lambda)$, for different k, Hodgkin-Huxley values of the parameters, all temperatures.

1. no asymmetric equilibria
   $-0.29577 < k$
   A simple computation with **Maple** shows that in this range $F(x) - kx$ has no critical points, being strictly monotonic (figure 1). There are no nontrivial solutions $x_1 \neq x_2$ for (1). For $k > -0.29577$, the function $F(x) - kx$ is strictly decreasing, with $\lim_{x\to+\infty} F(x) - kx = -\infty$ and $\lim_{x\to-\infty} F(x) - kx = +\infty$.
2. supercritical and subcritical pitchforks
   $-0.297 < k < -0.29577$
   In this range $F(x) - kx$ has two critical points, a local maximum and a local minimum (figure 4). Asymmetric equilibria exist only for a closed interval in the parameter μ. See figure 7.
3. two supercritical pitchforks and a secondary bifurcation (fold)
   $-g_0 = -0.3 < k < -0.297$
   There are still two critical points for $F(x) - kx$, a local maximum and a local minimum (figure 4). The two branches bifurcating from the symmetric

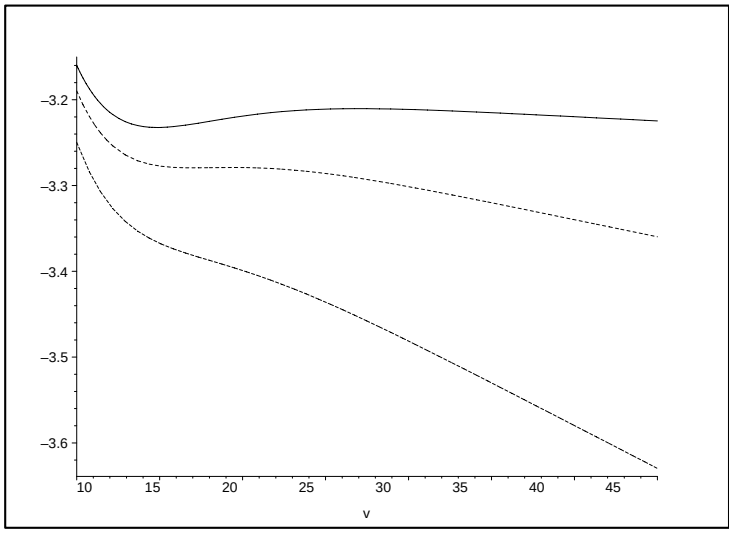

FIGURE 4. Graph of $F(x) - kx = f(x, \gamma(x)) - kx$ for $k = -0.299$ (full line); $k = -0.296$ (dotted); $k = -0.290$ (dashed), Hodgkin-Huxley values of the parameters.

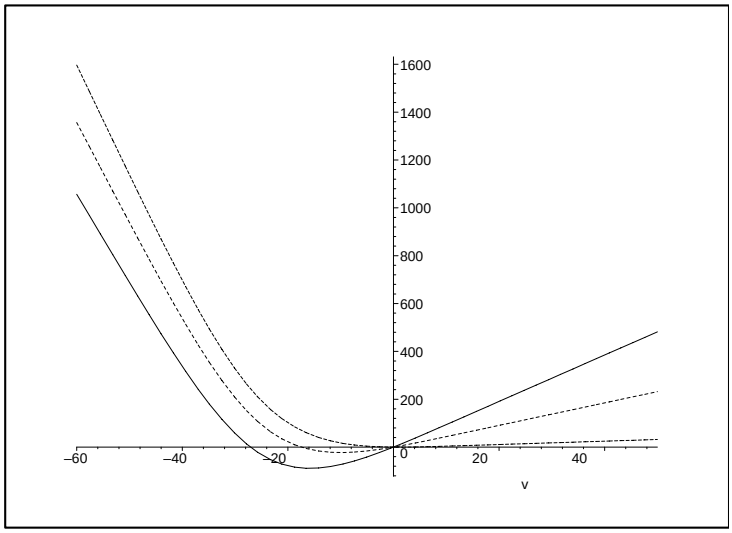

FIGURE 5. Graph of $F(x) - kx = f(x, \gamma(x)) - kx$ for $k = -10.0$ (full line); $k = -5.0$ (dotted); $k = -1.0$ (dashed), Hodgkin-Huxley values of the parameters.

equilibrium come together at fold points. Asymmetric equilibria exist only for a closed interval in the parameter μ. See figure 7

4. supercritical pitchfork
   $-0.4 \leq k < -0.3 = -g_0$
   In this range $F(x) - kx$ has a global minimum, say at $x = x_{min}$ and no other

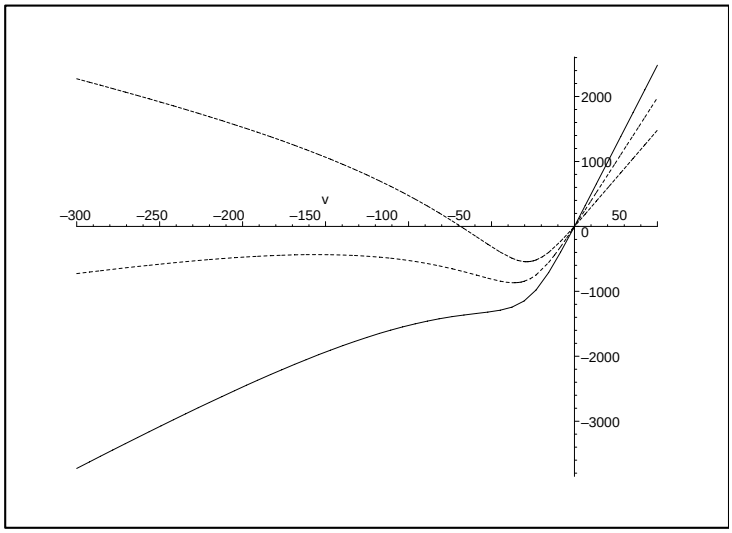

FIGURE 6. Graph of $F(x) - kx = f(x, \gamma(x)) - kx$ for $k = -50.0$ (full line); $k = -40.0$ (dotted); $k = -30.0$ (dashed), Hodgkin-Huxley values of the parameters.

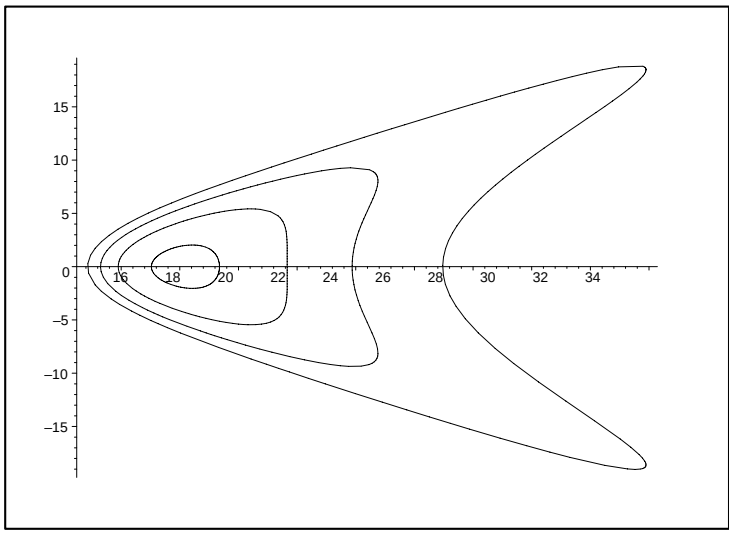

FIGURE 7. Bifurcation for **CHH**: position of asymmetric equilibrium $(\lambda, x_1 - \lambda)$, solution of (1) and (2), for different k, Hodgkin-Huxley values of the parameters, all temperatures. More negative values of k correspond to larger solution curves: $k = -0.296$ (case 2), smallest curve; $k = -0.297$; $k = -0.298$ (case 3); $k = -0.299$ (case 3), largest curve.

critical point. Thus, given $x_1 \neq x_{min}$ there is exactly one solution $x_2 \neq x_1$ for the equation (1). See figure 8.

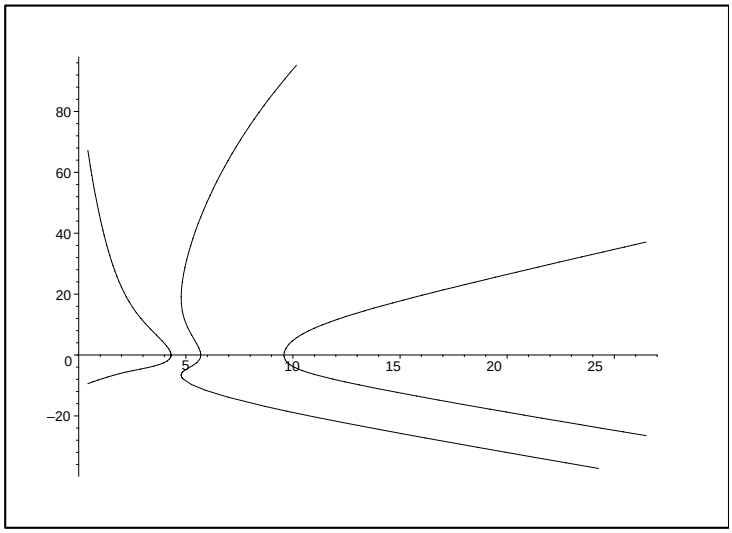

FIGURE 8. Bifurcation for **CHH**: position of asymmetric equilibrium $(\lambda, x_1 - \lambda)$, solution of (1) and (2), for different k, Hodgkin-Huxley values of the parameters, all temperatures. From left to right: $k = -0.6$ (case 6); $k = -0.5$ (case 5); $k = -0.35$ (case 4).

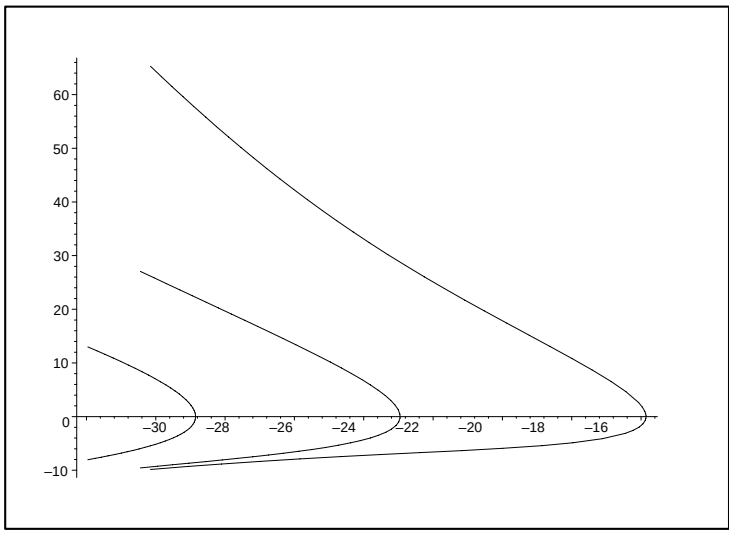

FIGURE 9. Bifurcation for **CHH**: position of asymmetric equilibrium $(\lambda, x_1 - \lambda)$, solution of (1) and (2), for different k in case 6, Hodgkin-Huxley values of the parameters, all temperatures. From left to right: $k = -30.0$; $k = -20.0$; $k = -10.0$.

5. subcritical pitchfork with secondary bifurcation (fold)
   $-2g_0(g_0 + g_2)/(2g_0 + g_2) = -0.59508 < k \leq -0.405$

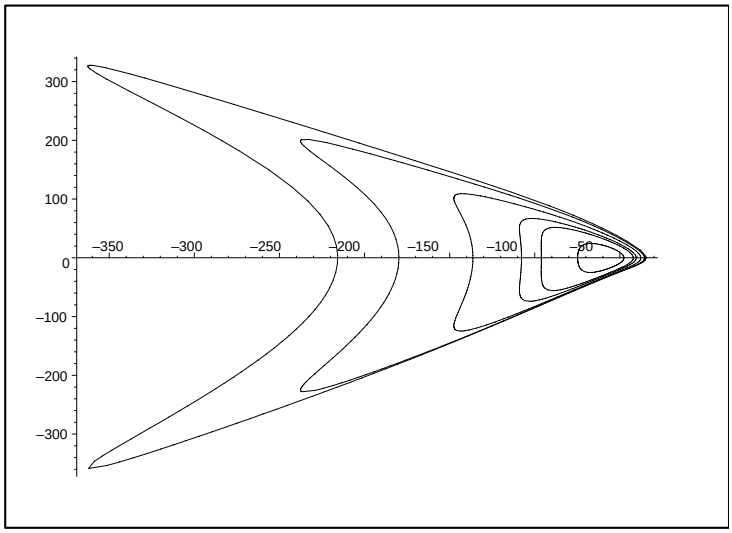

FIGURE 10. Bifurcation for **CHH**: position of asymmetric equilibrium $(\lambda, x_1 - \lambda)$, solution of (1) and (2), for different k, Hodgkin-Huxley values of the parameters, all temperatures. More negative values of k correspond to smaller solution curves: $k = -46.0$ (case 8) smallest curve; $k = -44.0$. Case 7: $k = -43.0$; $k = -41.0$; $k = -39.0$; $k = -38.0$, largest curve.

Again, $F(x) - kx$ has a global minimum and no other critical point. See figure 8.

6. subcritical pitchfork
   $-(g_0 + g_2) = -36.3 < k < -0.59508 = -2g_0(g_0 + g_2)/(2g_0 + g_2)$
   The only critical point of $F(x) - kx$ is a global minimum (figure 5). Figures 8 and 9.
7. two subcritical pitchforks and a secondary bifurcation (fold)
   $-43.0 \leq k < -36.3 = -(g_0 + g_2)$
   In this range $F(x) - kx$ has two critical points, a local maximum and a local minimum (figure 6). The two branches bifurcating from the symmetric equilibrium come together at fold points. Asymmetric equilibria exist only for a closed interval in the parameter μ. See figure 10.
8. supercritical and subcritical pitchforks
   $-47.00961 < k \leq -43.5$
   In this range $F(x) - kx$ has two critical points, a local maximum and a local minimum (figure 6). Asymmetric equilibria exist only for a closed interval in the parameter μ. See figure 10.
9. no asymmetric equilibria
   $k < -47.00961$
   Again a simple computation with **Maple** shows that in this range $F(x) - kx$ is strictly increasing (figure 6). There are no nontrivial solutions $x_1 \neq x_2$ for (1). For $k < -47.00961$, we have $\lim_{x \to +\infty} F(x) - kx = \infty$ and $\lim_{x \to -\infty} F(x) - kx = -\infty$.

2.1. **Numerical and analytical methods.** Asymmetric equilibria only exist, by (1), if $F(x)-kx$ is not one-to-one, having at least one critical point. A direct calculation using the expressions for $\gamma_j(x)$ shows that the graph of $F(x)$ has asymptotes $-g_0(x-V_0)-g_2(x-V_2)$ as $x\to-\infty$, and $-g_0(x-V_0)$ as $x\to+\infty$. This means that the behaviour of the graph of $F(x)-kx$ near $\pm\infty$ changes at $k=-g_0-g_2$ and $k=-g_0$. When $-g_0-g_2<k<-g_0$, we have $\lim_{x\to\pm\infty}F(x)-kx=+\infty$ and therefore $F(x)-kx$ has a global minimum. For the Hodgkin-Huxley values of the parameters this range is $-36.3<k<-0.3$. However, outside of this range there are still some nontrivial solutions $x_1\neq x_2$ to equation (1).

The analysis of the previous paragraph covers cases 4, 5 and 6. Let $x=x_{min}$ be the global minimum of $F(x)-kx$, direct computations with **Maple** show that it has no other critical point for $-36.3<k<-0.3$. Thus, given $x_1\neq x_{min}$ there is exactly one solution $x_2\neq x_1$ for the equation (1), see figure 5. This solution $x_2=\psi(x_1)$ was computed numerically with Newton's method, using as initial guess for x_2 the symmetrical of x_1 with respect to x_{min}, ie, $2x_{min}-x_1$, with an estimated error of 10^{-8}, working with 15 digits. The use of smaller errors in the method was tried but was abandoned, as it did not seem to affect the final results. The parameter value for the equilibrium was then computed from equation (2) as $\mu=\eta(x_1)=F^{-1}\left(F(x_1)-\frac{k}{2}(x_1-\psi(x_1))\right)$, again using Newton's method for F^{-1} with the same precision, yelding the bifurcation diagrams of figures 8 and 9, the graph of

$$(\mu,w)=(\eta(x_1),x_1-\eta(x_1))\ .$$

For k in the range for cases 2, 3, 7, and 8, $F(x)-kx$ has two critical points, a local maximum and a local minimum, see figures 4 and 6. Nontrivial solutions of (1) only exist for x_1 in a closed interval. The method described above was adapted to compute, given x_1, the two branches of solutions x_2 of (1) that were both used to obtain the the diagrams in the plane (μ,w), figures 7 and 10.

2.2. **Transition diagrams.** The persistent diagrams are better understood when we analize the transition cases. Calculations for these transitions were sometimes done by an independent method and provide aditional evidence for what takes place. There are two types of transition: the first type corresponds to a local bifurcation of codimension 1 with $\mathbf{Z}_2$ symmetry (cf. Chapter VI of [5]); the second type of transition takes place at $\mu=\pm\infty$.

- Case 1 to 2 and 9 to 8 — creation of a limited branch of asymmetric equilibria
  This transition corresponds to the normal form $x(x^2+\lambda^2-a)=0$ (*isola center* in [5]). It takes place when $F(x)-kx$ acquires a pair of critical points (figure 4) at an inflection point. The inflection point of $F(x)-kx$ was computed numerically from the analytic expressions of $F(x)-kx$ and its derivatives, and was found at $(x,k)=(-57.99173,-47.00961)$ and $(x,k)=(18.07494,-0.29577)$.
- Case 2 to 3; case 8 to 7 and also case 4 to 5 — change in the direction of one of the bifurcations
  This transition corresponds to the normal form $x(x^3-\lambda+ax^2)=0$ (*hysteresis* transition in [5]). The direction of bifurcation changes, and this creates a secondary bifurcation - a fold in the diagram. It was observed directly in the bifurcation diagrams, as in figure 8, and its location is determined with very low precision.
- Case 3 to 4 and also case 6 to 7 — bifurcation at infinity
  The slope of one of the asymptotes of $F(x)-kx$ changes sign, as discussed

in 2.1 (figure 6). This means that the number of critical points of $F(x) - kx$ changes and also the number of different solutions to (1). One of the pitchforks, as well as a pair of folds, tends to $\mu = \pm\infty$.

- Case 4 to 6 — a pair of folds goes to infinity
  Inside the region where $F(x) - kx$ has a single critical point, the map $\eta(x_1)$ (section 2.1) has, for some k, a local maximum. At this transition, the local maximum tends to infinity. The expression for $\lim_{x\to\pm\infty} \eta'(x)$ can be computed analytically and the value of k for which the limit is zero is given by

$$k = \frac{-2g_0(g_0 + g_2)}{2g_0 + g_2} \approx -0.59508 \ .$$

3. Hopf bifurcation

The eigenvalues of L are those of H and of $H - kJ$. We are interested in eigenvalues leading to bifurcation, with zero real part. For the matrix H, the eigenvalues at an equilibrium point are already studied in [10]: for the Hodgkin-Huxley values of the parameters and temperatures below $T = 28.858^oC$, pure imaginary eigenvalues appear at two values of λ, where there are Hopf bifurcations. For $T = 6.3$ they correspond to the two vertical lines in figure 11. In what follows we study the eigenvalues of $H - kJ$.

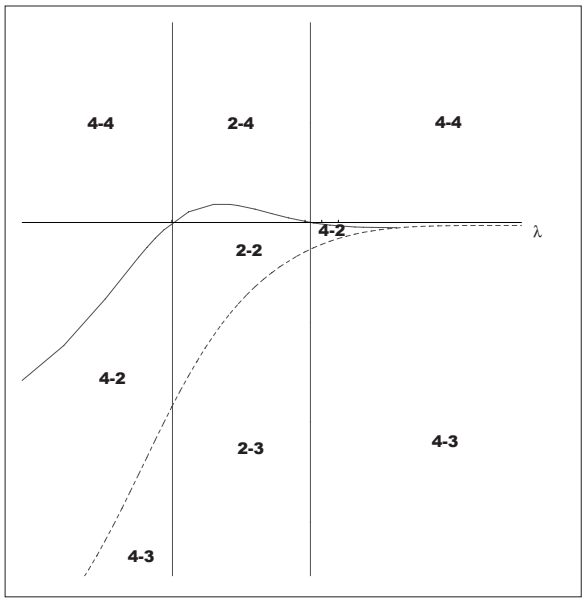

Figure 11. Stability of symmetric equilibrium for **CHH** in the $\lambda \times k$, plane for temperature $T = 6.3$, Hodgkin-Huxley values of the parameters. Full line, Hopf bifurcation, dashed line, pitchfork. The numbers m–n indicate eigenvalues with negative real part, m for H and n for $H - kJ$.

The polynomial $P_c(x)$ has a pair of conjugate pure imaginary roots, $\pm iw$, with $w \in \mathbf{R}$, if and only if the following relation on coefficients holds:

$$\Psi = c_0 c_3^2 - c_1 c_2 c_3 + c_1^2 = 0 \qquad \text{with} \qquad c_3 w^2 = c_1.$$

We have seen in section 1 that the coefficients c_j are affine in k. At a symmetric equilibrium, $\Psi(\lambda, k)$ is a polynomial of degree 3 in k.

The roots k of the polynomial $\Psi(\lambda, k)$ were computed with a program in $\mathbf{C}$ using the Cardano formula. The program then checks whether c_1 and c_3 have the same sign. The result, for $T = 6.3$, is shown in figure 11.

The direction of bifurcation was computed at points $(\lambda, k(\lambda))$ where we found a Hopf bifurcation. We used the method of [4] (see also [5]): after Liapunov-Schmidt reduction, the periodic solutions correspond to zeros of a function $xa(x^2, \lambda)$, with λ, and the derivatives of $a(u, \lambda)$, $u = x^2$ can be computed from those of the original system using the formulas of [3]. The bifurcation is *subcritical* if $a_u = \frac{\partial a}{\partial u}$ and $a_\lambda = \frac{\partial a}{\partial \lambda}$ have the same sign, *supercritical* otherwise. At points where any of these derivatives vanish we have a degenerate Hopf bifurcation. This is the case at the maximum of the graph of $\psi(\lambda, k) = 0$, since $-a_\lambda$ is the derivative of the real part of the eigenvalue undergoing bifurcation and therefore it is zero. See figure 12 graphs of a_λ.

In figure 13 it can be seen that a_u changes sign three times. These degenerate Hopf bifurcation points are discussed in section 4.

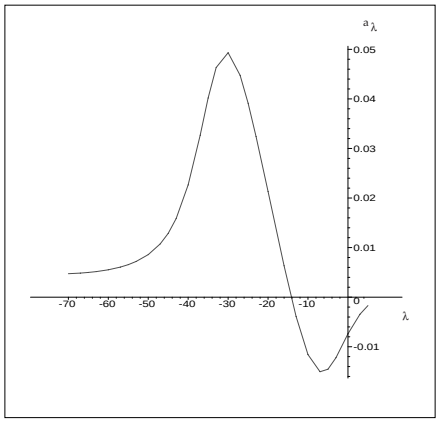

FIGURE 12. a_λ for $T = 6.3$, with λ in the interval where there is a Hopf bifurcation, $k = k(\lambda)$, Hodgkin-Huxley values of remaining parameters.

4. Bifurcation diagrams

In this section we describe the structures arising through the bifurcations we have found. For each parameter value there may be the following: the unique symmetric equilibrium $(\lambda, \gamma(\lambda), \lambda, \gamma(\lambda))$; one or two symmetric periodic solutions of the form $(X(t), X(t))$, $X(t) \in \mathbf{R}^4$; one or two pairs of asymmetric equilibria of the form (X, Y) and (Y, X). Hopf bifurcation from the symmetric equilibrium in the asymmetric direction gives rise to asymmetric periodic solutions $(X(t), Y(t))$. In this case the set $\{(X(t), Y(t)) \quad t \in \mathbf{R}\}$ is $\mathbf{Z}_2$-invariant although the solutions

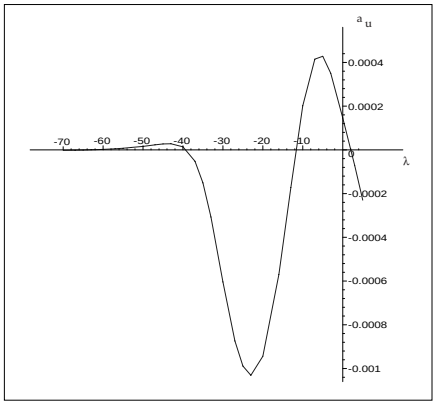

FIGURE 13. a_u for $T = 6.3$, with λ in the interval where there is a Hopf bifurcation, $k = k(\lambda)$, Hodgkin-Huxley values of remaining parameters.

are not. More complicated solutions appear at secondary bifurcations: symmetry related pairs of asymmetric periodic solutions, and invariant torii. These more complicated structures seem to be always unstable, we only discuss them for the sake of completeness.

How these structures appear with varying stability is described in figures 15 and 14. These are very distorted — as usual, most things happen in a minute portion of parameter space, as can be seen comparing figure 14 to the realistic plots figure 2 (pitchfork locus) and in figure 11.

For each region in the diagrams we indicate the structures arising through bifurcation, and their stability. The numbers (m–n) indicate, for an equilibrium point, the number of eigenvalues with negative real part, m for H and n for $H - kJ$. For a periodic orbit (m–n) indicates the dimension of the stable manifold, components in the (X, X) and $(X, -X)$ directions, respectively. Although at an asymmetric point these subspaces are no longer invariant by the matrix L of the linearization, near the symmetric points the eigenspaces of L are still close to them.

4.1. **Codimension one bifurcations.** These correspond to curves and lines in figures 14 and 15 and are:
Ho-s = symmetric Hopf bifurcation;
Ho = asymmetric Hopf bifurcation;
pf = pitchfork;
sn = saddle-node of asymmetric equilibria.
in = a pair of saddle-nodes goes to $-\infty$;
dl-a = asymmetric double loop (saddle-node of periodic orbits);
dl-s = symmetric double loop(saddle-node of periodic orbits);
he = heteroclinic connection of a pair of asymmetric equilibria;
sb = secondary bifurcation (see mode interaction, below);

The first four types in the list above (**Ho-s**, **Ho**, **pf**, **sn**) were found numerically (full lines), the last four (**dl-a**, **dl-s**, **he**, **sb**) were obtained from the presence of codimension 2 points and are discussed below.

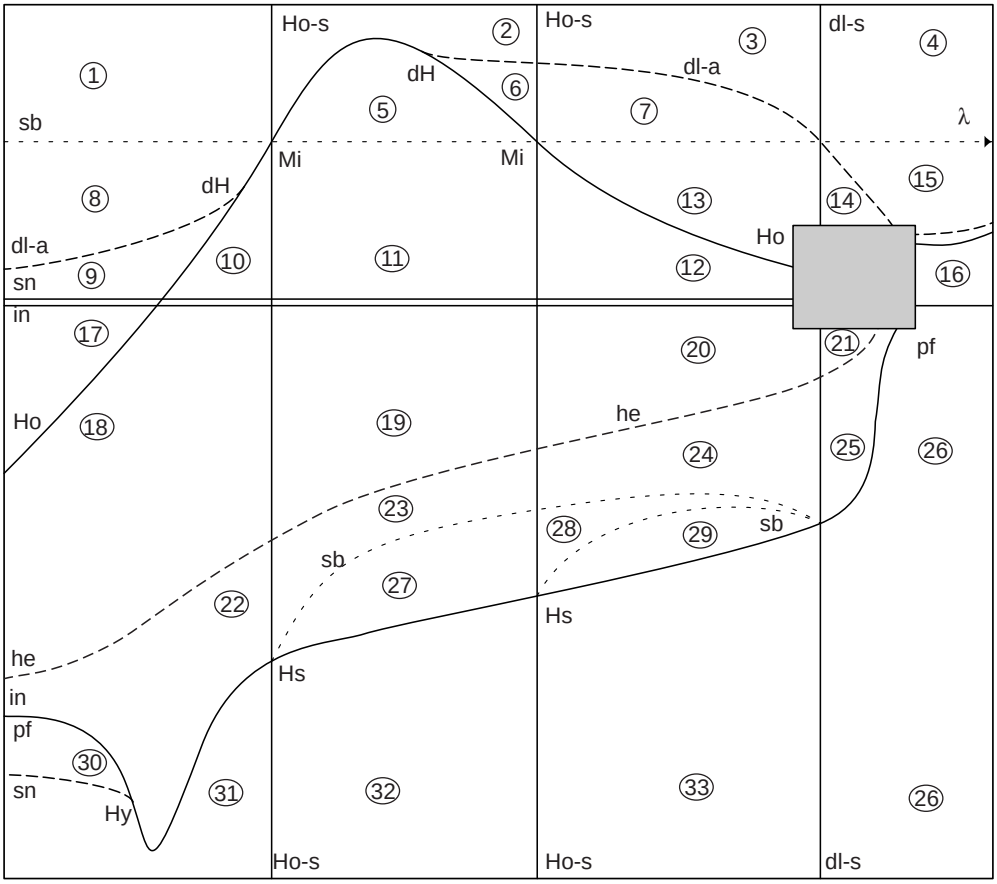

FIGURE 14. Qualitative bifurcation diagram for **CHH** in the $\lambda \times k$ plane for temperature $T = 6.3$. Behaviour for regions 1–33 described below. Gray rectangle corresponds to figure 15. Full lines were found numerically; dashed lines added to complete the diagram. Identification of lines and codimension 2 points, in the text.

At the horizontal line $k = -2g_0(g_0 + g_2)/(2g_0 + g_2)$, the bifurcation labelled **in**, a pair of asymmetric saddle-nodes tends to $\lambda = -\infty$ as discussed in section 2. The curve of saddle-nodes **sn** approaches this line asymptotically.

4.2. **Codimension 2 bifurcations.** We have found the following bifurcations, for detailed description see [8] and [5]:
dH = degenerate Hopf bifurcation
On the curve of asymmetric Hopf bifurcation there are three of these points, (two represented in figure 14 and one in 15) where the direction of the bifurcation changes (see figure 13). The two periodic solutions created at the Hopf bifurcation come together at the curve of asymmetric double loops labelled **dl-a**. A similar bifurcation takes place for the uncoupled Hodgkin and Huxley equations when the parameter g_1 is varied, giving rise to the line of symmetric double loops **dl-s** [10].

Hy = hysteresis
At three points on the curve of pitchforks (one in figure 14 and two in figure 15) the direction of bifurcation changes. A curve of asymmetric saddle-nodes **sn** originates at each of these points.
T = symmetric Takens bifurcation
This bifurcation ocurs at a point where the linearization has a double zero eigenvalue, in equations with $\mathbf{Z}_2$ symmetry, it is a $\mathbf{Z}_2$-equivariant version of Bogdanov-Takens bifurcation, see [8]. A curve of Hopf bifurcations (**Ho**) and a curve of heteroclinic connections (**he**) terminate at the curve of pitchforks (figure 15).
Mi = Hopf/Hopf mode interaction
Two points where there are symmetric and asymmetric Hopf bifurcation at the same place, discussed in 4.5 below.
Hs = Hopf/steady-state mode interaction
Two points where the curve of pitchforks crosses the two lines of symmetric Hopf bifurcation at the same place, discussed in 4.5 below.

4.3. **Structures arising through the bifurcations in diagram of figure 14 .** We describe the structures by horizontal bands, repeating the cases **1** to **10** when necessary, for ease of interpretation.

Structures for $k > 0$, large :

region **(1)**
1 symmetric equilibrium, stable (4–4)

region **(2)**
1 symmetric equilibrium, unstable (2–4)
1 symmetric periodic solution, stable (4–4)

region **(3)**
1 symmetric equilibrium, stable (4–4)
2 symmetric periodic solutions, one stable (4–4), one unstable (3–4)

region **(4)**
1 symmetric equilibrium, stable (4–4)

Structures for $k > 0$, small:

region **(1)**
1 symmetric equilibrium, stable (4–4)

region **(2)**
1 symmetric equilibrium, unstable (2–4)
1 symmetric periodic solution, stable (4–4)

region **(5)**
1 symmetric equilibrium, unstable (2–2)
1 symmetric periodic solution, stable (4–4)
1 asymmetric periodic solution, unstable (2–4)

region **(6)**
1 symmetric equilibrium, unstable (2–4)
1 symmetric periodic solution, stable (4–4)
2 asymmetric periodic solutions, unstable (2–4) and (2–3)

region **(7)**
1 symmetric equilibrium, stable (4–4)
2 symmetric periodic solutions, one stable (4–4), one unstable (3–4)
2 asymmetric periodic solutions, unstable (2–4) and (2–3)

region **(3)**
1 symmetric equilibrium, stable (4–4)
2 symmetric periodic solutions, one stable (4–4), one unstable (3–4)

region **(4)**
1 symmetric equilibrium, stable (4–4)

Although the axis $k = 0$ is not a bifurcation line, the stability of equilibria and periodic solutions changes between adjacent regions **5** and **11** and also from region **7** to **13**. These bifurcations are organized by Hopf/Hopf mode interactions that will be discussed in 4.5 below.

Structures for $k < 0$, near the axis (besides structures in gray rectangle, figure 15):

region **(8)**
1 symmetric equilibrium, stable (4–4)

region **(9)**
1 symmetric equilibrium, stable (4–4)
2 asymmetric periodic solutions, one stable (4–4) and one unstable (4–3)

region **(10)**
1 symmetric equilibrium, unstable (4–2)
1 asymmetric periodic solution, stable (4–4)

region **(11)**
1 symmetric equilibrium, unstable (2–2)
1 symmetric periodic solution, unstable (4–2)
1 asymmetric periodic solution, stable (4–4)

region **(12)**
1 symmetric equilibrium, unstable (4–2)
2 symmetric periodic solutions, unstable (4–2) and (3–2)
1 asymmetric periodic solution, stable (4–4)

region **(13)**
1 symmetric equilibrium, stable (4–4)
2 symmetric periodic solutions, unstable (4–2) and (3–2)
2 asymmetric periodic solutions, one stable (4–4), one unstable (4–3)

region **(14)**
1 symmetric equilibrium, stable (4–4)
2 asymmetric periodic solutions, one stable (4–4), one unstable (4–3)

region **(15)**
1 symmetric equilibrium, stable (4–4)

region **(16)**
1 symmetric equilibrium, unstable (4-3)
1 pair of asymmetric equilibria, stable (4–4)

Structures for $k < 0$, below line of bifurcation at infinity:

region **(17)**
1 symmetric equilibrium, stable (4–4)
2 asymmetric periodic solutions, one stable (4–4) and one unstable (4–3)
1 pair of asymmetric equilibria, unstable (4–3)

region **(18)**
1 symmetric equilibrium, unstable (4–2)
1 asymmetric periodic solution, stable (4–4)
1 pair of asymmetric equilibria, unstable (4–3)

region **(19)**
1 symmetric equilibrium, unstable (2–2)
1 symmetric periodic solution, unstable (4–2)
1 asymmetric periodic solution, stable (4–4)
1 pair of asymmetric equilibria, unstable (4–3)

region **(20)**
1 symmetric equilibrium, unstable (4–2)
2 symmetric periodic solutions, unstable (4–2) and (3–2)
1 asymmetric periodic solution, stable (4–4)
1 pair of asymmetric equilibria, unstable (4–3)

region **(21)**
1 symmetric equilibrium, unstable (4–2)
1 asymmetric periodic solution, stable (4–4)
1 pair of asymmetric equilibria, unstable (4–3)

Structures for $k < 0$, below line of heteroclinic connection:

region **(22)**
1 symmetric equilibrium, unstable (4–2)
1 pair of asymmetric equilibria, unstable (4–3)

region **(23)**
1 symmetric equilibrium, unstable (2–2)
1 symmetric periodic solution, unstable (4–2)
1 pair of asymmetric equilibria, unstable (4–3)

region **(24)**
1 symmetric equilibrium, unstable (4–2)
2 symmetric periodic solutions, unstable (4–2) and (3-2)
1 pair of asymmetric equilibria, unstable (4–3)

region **(25)**
1 symmetric equilibrium, unstable (4–2)
1 pair of asymmetric equilibria, unstable (4–3)

region **(26)**
1 symmetric equilibrium, unstable (4-3)

Structures for $k < 0$, after secondary bifurcations:

region **(27)**
1 symmetric equilibrium, unstable (2–2)
1 symmetric periodic solution, unstable (4–3)
1 pair of asymmetric equilibria, unstable (2–3)

region **(28)**
1 symmetric equilibrium, unstable (4–2)
2 symmetric periodic solutions, unstable (4–3) and (3–2)
1 pair of asymmetric equilibria, unstable (2–3)

region **(29)**
1 symmetric equilibrium, unstable (4–2)
2 symmetric periodic solutions, unstable (4–3) and (3–3)
1 pair of asymmetric equilibria, unstable (4–3)

Structures for $k << 0$, lower end of diagram

region **(30)**
1 symmetric equilibrium, unstable (4–3)
2 pairs of asymmetric equilibria, unstable (4–3) and (4–2)

region **(24)**
1 symmetric equilibrium, unstable (4–2)
1 pair of asymmetric equilibria, unstable (4–3)

region **(31)**
1 symmetric equilibrium, unstable (4-3)

region **(32)**
1 symmetric equilibrium, unstable (2–3)
1 symmetric periodic solution, unstable (4–3)

region **(33)**
1 symmetric equilibrium, unstable (4–3)
2 symmetric periodic solutions, unstable (4–3) and (3-3)

region **(26)**
1 symmetric equilibrium, unstable (4-3)

4.4. **Structures arising through the bifurcations in diagram for the detail, figure 15.** Again, we proceed by horizontal strips. Regions near the top line of the figure:

region **(12)**
1 symmetric equilibrium, unstable (4–2)
2 symmetric periodic solutions, unstable (4–2) and (3–2)
1 asymmetric periodic solution, stable (4–4)

region **(13)**
1 symmetric equilibrium, stable (4–4)
2 symmetric periodic solutions, unstable (4–2) and (3–2)
2 asymmetric periodic solutions, one stable (4–4), one unstable (4–3)

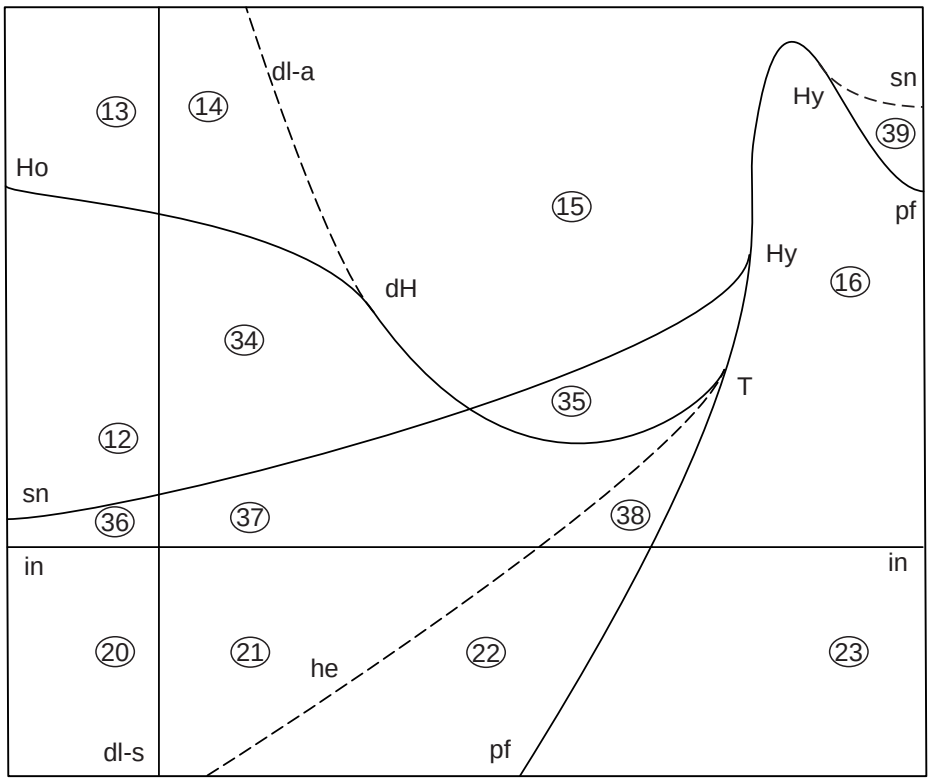

FIGURE 15. Detail of qualitative bifurcation diagram for **CHH** in the $\lambda \times k$ plane for temperature $T = 6.3$. Behaviour for regions described by number in the text. Full lines were found numerically; dashed lines added to complete the diagram. Conventions for lines and codimension 2 points in the text.

region **(14)**
1 symmetric equilibrium, stable (4–4)
2 asymmetric periodic solutions, one stable (4–4), one unstable (4–3)

region **(15)**
1 symmetric equilibrium, stable (4–4)

region **(16)**
1 symmetric equilibrium, unstable (4-3)
1 pair of asymmetric equilibria, stable (4–4)

region **(39)**
1 symmetric equilibrium, stable (4–4)
2 pairs of asymmetric equilibria, 1 pair stable (4–4) and one unstable (4–3)

Structures below the top line of the diagram:

region **(12)**
1 symmetric equilibrium, unstable (4–2)
2 symmetric periodic solutions, unstable (4–2) and (3–2)
1 asymmetric periodic solution, stable (4–4)

region **(34)**
1 symmetric equilibrium, unstable (4–2)
1 asymmetric periodic solution, stable (4–4)

region **(15)**
1 symmetric equilibrium, stable (4–4)

region **(35)**
1 symmetric equilibrium, stable (4–4)
2 pairs of asymmetric equilibria, one stable (4–4), one unstable (4–3)

region **(16)**
1 symmetric equilibrium, unstable (4-3)
1 pair of asymmetric equilibria, stable (4–4)

Structures above the line of bifurcation at infinity:

region **(36)**
1 symmetric equilibrium, unstable (4–2)
2 symmetric periodic solutions, unstable (4–2) and (3–2)
1 asymmetric periodic solution, stable (4–4)
2 pairs of asymmetric equilibria, one stable (4–4), one unstable (4–3)

region **(37)**
1 symmetric equilibrium, unstable (4–2)
1 asymmetric periodic solution, stable (4–4)
2 pairs of asymmetric equilibria, one stable (4–4), one unstable (4–3)

region **(38)**
1 symmetric equilibrium, unstable (4–2)
2 pairs of asymmetric equilibria, one stable (4–4), one unstable (4–3)

region **(16)**
1 symmetric equilibrium, unstable (4-3)
1 pair of asymmetric equilibria, stable (4–4)

Structures along the bottom of the diagram:

region **(20)**
1 symmetric equilibrium, unstable (4–2)
2 symmetric periodic solutions, unstable (4–2) and (3–2)
1 asymmetric periodic solution, stable (4–4)
1 pair of asymmetric equilibria, unstable (4–3)

region **(21)**
1 symmetric equilibrium, unstable (4–2)
1 asymmetric periodic solution, stable (4–4)
1 pair of asymmetric equilibria, unstable (4–3)

region **(22)**
1 symmetric equilibrium, unstable (4–2)
1 pair of asymmetric equilibria, unstable (4–3)

region **(23)**
1 symmetric equilibrium, unstable (4-3)

4.5. **Mode interaction .** Consider the point labelled **Mi** on the upper left hand part of figure 14, where the curve of asymmetric Hopf bifurcations crosses the line of symetrical Hopf bifurcations. For fixed k all the bifurcations near this point are supercritical in the parameter λ. At region **(1)** there is only a stable symmetric equilibrium. As λ increases, the symmetric equilibrium loses stability at two successive Hopf bifurcations. For $k > 0$ we get a stable symmetric periodic solution in region **(5)**. The symmetric periodic solution is unstable in the corresponding region, **(11)**, for $k < 0$. At the same time, the asymmetric periodic solution gains stability when we move from **(5)** to **(11)**. Thus, near the $k = 0$ axis, there must be some bifurcation where the stability of both types of periodic solution changes. Similar situations arise near the other point labelled **Mi**, and near both points labeled **Hs**.

What is taking place is called a *mode interaction with symmetry* — a Hopf/Hopf mode interaction at **Mi** (two "independent" Hopf bifurcations at the same point) or a Hopf/steady-state mode interaction at **Hs** (a Hopf bifurcation and a pitchfork at the same point). For a discussion of the complicated dynamics that may arise in the non-symmetric case, see for instance chapter 7 of [8]. In our case, since we start wih a system with symmetry, both types of bifurcation may be reduced — after a suitable choice of coordinates and passing to loop space (see [7]) — to steady-state bifurcations with $\mathbf{Z}_2 + \mathbf{Z}_2$ symmetry, in two dimensional phase space. These are studied in Chapter X of [5].

Returning to the upper left hand part of figure 14, there are two of *modes*, here identified to the two types of periodic solution, symmetric and asymmetric. The secondary bifurcations may give rise to *mixed modes*, in our case, invariant torii. Starting with (λ, k) in region **(5)** and keeping λ fixed, we describe a possible sequence of secondary bifurcations taking place as we decrease k until we're well into region **(11)**. Different sequences of bifurcations may fit in this picture, as shown in Chapter X of [5], but since we are interested in stable structures, we explore the only scenario where these are generated: first a supercritical Hopf bifurcation at the stable symmetric periodic solution, creating a stable branch of mixed modes, followed by a subcritical bifurcation of the asymmetric periodic solution, where the mixed modes are destroyed. Any other scenario will give rise to unstable structures. Since no evidence of stable torii was fond in numerical simulations on this region, we conclude that this scenario does not apply. Therefore the secondary bifurcations yeld unstable modes. The same discussion applies the similar bifurcation at the other **Mi** point, except that, as we are starting with unstable modes, no scenario will give rise to stable mixed modes.

A similar discussion covers the cases of the two points labelled **Hs** in figure 14. Here one of the modes is a symmetric periodic solution and the other a symmetry related pair of asymmetric equilibria. Mixed modes correspond to a pair of symmetry related asymmetric periodic orbits. However, since both modes are unstable

to start with, it follows that the mixed modes will also be unstable, and there is no point in pursuing the analysis any further.

References

[1] Buono P-L., Golubitsky M., *Models of central pattern generators for quadruped locomotion I. Primary gaits*, J. Mathematical Biology, **42**, 291–326, (2001)

[2] Buono P-L., *Models of central pattern generators for quadruped locomotion II. Secondary gaits*, J. Mathematical Biology, **42**, 291–326, (2001)

[3] Farr, W.W., Li, C., Labouriau, I.S., Langford,W.F., *Degenerate Hopf bifurcation formulas and Hilbert's 16th problem*, SIAM J. Math Anal., **20**, 13–30 (1989)

[4] Golubitsky, M., Langford, W. F. , *Classification and unfoldings of degenerate Hopf bifurcations*, J. Diff. Eqns, **41**, 375–415, (1981)

[5] Golubitsky, M., Schaeffer, D.G., *Singularities and groups in bifurcation theory, volume I* Springer-Verlag (1984)

[6] Golubitsky, M., Stewart, I., Schaeffer, D.G., *Singularities and groups in bifurcation theory, volume II* Springer-Verlag (1987)

[7] Golubitsky, M., Stewart, I., *The symmetry perspective: From Equilibrium to Chaos in Phase Space and Physical Space* Birkhauser, Basel (2002)

[8] Guckenheimer J., Holmes P., *Nonlinear oscillations, dynamical systems and bifurcations of vector fields*, Springer-Verlag (1983)

[9] Hodgkin A.L., Huxley, A.F., *A quantitative description of membrane current and its application to conduction and excitation in nerve*, Journal of Physiology, vol **117** pp 500–544, 1952. Reproduced in Bulletin of Mathematical Biology, **52**, 25–71, (1990)

[10] Labouriau. I.S., *Degenerate Hopf bifurcation and nerve impulse*, SIAM J. Math Anal., **16**, 61–71 (1985)

[11] Labouriau I.S., Pinto C.M.A., *Loss of Synchronization in Partially Coupled Hodgkin-Huxley Equations*, preprint, (2003)

[12] Labouriau I.S., Rodrigues H.S., *Synchronization of coupled equations of Hodgkin-Huxley type*, Dynamics of Continuous, Discrete and Impulsive Systems (2003) Series A — Mathematical Analysis, **10 A**, 463–476

[13] Pinto C.M.A., PhD Tesis, Universidade do Porto, Portugal, in preparation.

I.S.Labouriau — Centro de Matemática da Universidade do Porto, Rua do Campo Alegre, 687, 4169-007 Porto, Portugal

E-mail address: islabour@fc.up.pt

C.M.A.Pinto — Departamento de Matemática Aplicada, Faculdade de Ciências, Universidade do Porto, Rua do Campo Alegre, 687, 4169-007 Porto, Portugal

E-mail address: cap@isep.ipp.pt